*Arabidopsis* RAD23B regulates pollen development by mediating KRP1 degradation

Lan Li, E-mail: lilan7@hnu.edu.cn

Bin Li, E-mail: binli369@hnu.edu.cn

Chong Xie, E-mail: xiechong7@hnu.edu.cn

Teng Zhang, E-mail: zhangtengteng@hnu.edu.cn

Cecilia Borassi, E-mail: cborassi@leloir.org.ar

**Corresponding Authors:**

Estevez JM, E-mail: jestevez@leloir.org.ar / jose.estevez@unab.cl

XS Li, E-mail: lxs812_88@163.com

XM Liu, E-mail: xmL05@hnu.edu.cn, 0731-88821721

State Key Laboratory of Chemo/Biosensing and Chemometrics and Hunan Key Laboratory of Plant Functional Genomics and Developmental Regulation.

College of Biology, Hunan University, Changsha 410082, P. R. China.

Fundación Instituto Leloir-IIBBA, Av. Patricias Argentinas 435, Buenos Aires CP C1405BWE, Argentina.

Centro de Biotecnología Vegetal, Facultad de Ciencias de la Vida, Universidad Andres Bello, Santiago, Chile and Millennium Institute for Integrative Biology (iBio), Santiago, Chile.

Accepted Manuscript

Downloaded from https://academic.oup.com/jxb/advance-article-abstract/doi/10.1093/jxb/eraa167/5815313 by guest on 07 April 2020

© The Author(s) 2020. Published by Oxford University Press on behalf of the Society for Experimental Biology.

This is an Open Access article distributed under the terms of the Creative Commons Attribution License (http://creativecommons.org/licenses/by/4.0/), which permits unrestricted reuse, distribution, and reproduction in any medium, provided the original work is properly cited.

Lan Li[1*], Bin Li[1*], Chong Xie[1], Teng Zhang[1], Cecilia Borassi[2], Estevez JM[2,3#], Xiushan Li[1#], Xuanming Liu[1#]

[1] College of Biology, State Key Laboratory of Chemo/Biosensing and Chemometrics and Hunan Key Laboratory of Plant Functional Genomics and Developmental Regulation Hunan University, Changsha 410082, P. R. China.

[2]Fundación Instituto Leloir and IIBBA-CONICET, Av. Patricias Argentinas 435, Buenos Aires CP C1405BWE, Argentina.

[3]Centro de Biotecnología Vegetal, Facultad de Ciencias de la Vida, Universidad Andres Bello, Santiago, 8370186, Chile and Millennium Institute for Integrative Biology (iBio), Santiago, 8331150, Chile.

[*]These authors contributed equally to this work.

[#] Corresponding Authors: E-mail: xmL05@hnu.edu.cn, Fax: 86-731-8882-2606. E-mail: lxs812_88@163.com, E-mail: jestevez@leloir.org.ar / jose.estevez@unab.cl.

Accepted Manuscript

Downloaded from https://academic.oup.com/jxb/advance-article-abstract/doi/10.1093/jxb/eraa167/5815313 by guest on 07 April 2020

**Highlight**

RAD23B as a UBL/UBA protein contributes to KRP1 degradation, and *rad23b* mutants and overexpress plants of *KRP1*exhibit pollen development defects.

Accepted Manuscript

Downloaded from https://academic.oup.com/jxb/advance-article-abstract/doi/10.1093/jxb/eraa167/5815313 by guest on 07 April 2020

**Abstract**

The ubiquitin (Ub)/26S proteasome system (UPS) plays a key role in plant growth, development, and survival by directing the turnover of numerous regulatory proteins. In UPS, ubiquitin-like (UBL) and ubiquitin-associated (UBA) domains function as hubs for ubiquitin-mediated protein degradation. RADIATION SENSITIVE23 (RAD23), which was identified as a UBL/UBA protein, contributed to cell cycle progression, stress response, ER proteolysis, and DNA repair. Here, we report pollen is arrested at the microspore stage in a null *rad23b* mutant. We demonstrated that RAD23B can directly interact with KIP-RELATED PROTEIN 1 (KRP1) through its UBL-UBA domains. In addition, overexpression plants of *KRP1* resulted in pollen development defects, a phenotype similar to the *rad23b* mutant. Finally, RAD23B was found to promote the degradation of KRP1 *in vivo*, which was accumulated following treatment with MG132. In summary, these results indicate the important role of RAD23B in pollen development by controlling turnover of a key cell cycle protein, KRP1.

**Keywords:** cell cycle, KRP1, pollen abortion, proteasome system, RAD23B, ubiquitin.

Accepted Manuscript

Downloaded from https://academic.oup.com/jxb/advance-article-abstract/doi/10.1093/jxb/eraa167/5815313 by guest on 07 April 2020

**Abbreviations**

CDKs, cyclin-dependent kinases;

DSK2, dominant suppressor of KAR2;

GUS, β-glucuronidase;

ICKs, interactors of Cdc2 Kinase;

KRPs, kip-related proteins;

UBA, ubiquitin-associated;

UBL, ubiquitin-like;

UPS, ubiquitin-proteasome system;

Y2H, Yeast 2 hybrid;

Accepted Manuscript

Downloaded from https://academic.oup.com/jxb/advance-article-abstract/doi/10.1093/jxb/eraa167/5815313 by guest on 07 April 2020

## Introduction

In eukaryotes, the ubiquitin (Ub)/26S proteasome system (UPS) controls protein degradation by orchestrated targeting, ubiquitin labeling, and degradation of proteins. UPS plays a vital role in many biological processes such as plant growth (shen *et al.,* 2005), development (Jasmina *et al.,* 2009), and survival (Du *et al*., 2009). Ubiquitin-like (UBL) and ubiquitin-associated (UBA) domains function as hubs during ubiquitin-mediated protein degradation (Lowe *et al*., 2006). Although the importance of UPS in substrate recognition is widely known, the function of UBL/UBA proteins in the plant kingdom remains elusive (Bethan *et al*., 2011). In animals, Radiation sensitive 23 (RAD23), which was identified as a UBL/UBA protein, contains an amino-terminal UBL domain and two UBA domains (Andersson *et al.,* 2005). Díaz-Martínez et al. showed that RAD23 played an important role in the cell-cycle regulation (Díaz-Martínez *et al*., 2006). Knockout of RAD23 was shown to inhibit cell growth (Hänzelmann *et al*., 2010). In plants, *rad23b* mutants display pleiotropic developmental defect, abnormal phyllotaxy, shorter primary root, unfertilized ovules, smaller siliques and had reduced seed set (Farmer *et al*., 2010). Meanwhile, it has been reported that RAD23 regulated plant development, presumably by delivering target proteins to the UPS (Liang *et al*., 2014).

The regulation mechanisms of cell cycle, which can be divided into four phases of G1, S, G2 and M, are highly conserved (Cross *et al.,* 2011). It has been shown that there are two major cell cycle checkpoints, the transition G1 phase prior to the initiation of S phase (G1-S transcription) and the transition from G2 phase into M phase (G2-M transcription) (Haase, S. B., and Wittenberg, C., 2014). Cellular cyclin-dependent kinases (CDKs) are important in cell cycle progression and cell division (Ding *et al*., 2005). CDK inhibitors (ICKs) can inhibit CDK activity through directly protein binding. Until now, seven CDK inhibitors have been identified in *Arabidopsis thaliana* (De Veylder *et al*., 2001; David A *et al*., 2007). Among them, the *KRP1* and *KRP2* transcript levels were significantly regulated by PRMT5 during shoot regeneration (Liu *et al.,* 2016). Moreover, ICK1/KRP1 and ICK2/KRP2 were observed to be regulated by the 26S proteasome (Weinl *et al.,* 2005; Lai *et al.,* 2010). KRP1 degradation was dependent both on SCF $^{SKP2b}$ and the RING protein RPK (Ren *et al.,* 2008). However, how KRPs proteins are degraded remains elusive.

In this study, it was found that the number of abnormal microspore development increased in the *rad23b* mutant. This phenotype is similar to the KRP1 overexpression plant. Furthermore, yeast 2 hybrid (Y2H) results demonstrated that RAD23B directly interacted with KRP1. In addition, we also found that RAD23B promoted the degradation of KRP1 *in vivo*. These data indicate that the interaction of RAD23B and KRP1 is essential for the degradation of KRP1 and the regulation of cell division. Thus, we speculate that RAD23B controls cell division by promoting KRPs degradation in pollen grains.



Accepted Manuscript

Downloaded from https://academic.oup.com/jxb/advance-article-abstract/doi/10.1093/jxb/eraa167/5815313 by guest on 07 April 2020

## Materials and Methods

### Plant materials and growth conditions.

All *Arabidopsis thaliana* mutants used in this study were derived from the Col-0 background. Mutants *rad23b-1* (Salk_075940) and *rad23b-2* (Salk_130110) were obtained from ABRC. The T-DNA insertion mutants were identified by PCR using primers *LP* and *RP* (Table S1). The T-DNA insertion site, as described in http://signal.salk.edu, was confirmed by PCR-based genotyping (Peng *et al.*, 2012; Zhang *et al.*, 2012). *Arabidopsis thaliana* seeds were stratified at 4°C for two days before being grown on ½-strength Murashige and Skoog media (1/2 MS) with 0.8% sucrose and 1% Phytagel (A7002, Sigma-Aldrich) for subsequent analysis. The resulting *Arabidopsis thaliana* mutants were grown under a 16 h-light and 8 h-dark cycle at 22°C.

#### Construction of transgenic plants.

Fragments of the *RAD23B* gene were amplified and cloned, using a gateway strategy, into the entry vector pDONR201. The coding sequence of *RAD23B* was then cloned into the destination vector *pENSG-GFP-GW*. In addition, *RAD23B* and *KRP1* genes were also cloned into the vector pDT1 using the primers of *RAD23B-pDT1-F*, *RAD23B-pDT1-R*, *KRP1-pDT1-F* and *KRP1-pDT1-R*, respectively. All of the resulting plasmids were used to transform *Agrobacterium tumefaciens* GV3101 by electroporation for delivery into *Arabidopsis thaliana* Col-0. The *rad23-b* mutant plants were created using the floral dip method (Clough and Bent, 1998). The transgenic plants were screened using the herbicide basta to identify homozygous lines. Leaves and flowers from the homozygous transgenic lines were collected and stored at -80°C. All the primers used here are presented in Table S1.

#### Total RNA extraction and RT-PCR.

Six 7-days-old *Arabidopsis thaliana* seedlings were chosen, randomly. Total RNA was isolated as described previously (Peng *et al.,* 2012), and reverse-transcribed to cDNA (Takara) after DNase treatment. The cDNA product was diluted 20 folds, and 0.5 µL of diluted cDNA was used in a 20 µL PCR reaction. The expression level of the *KRP1* gene was measured by RT-PCR for at least three independent experiments (*n*=3). The sequences of the RT-PCR-rad23b-1 and RT-PCR-rad23b-2 primers used in this study are listed in Table S1.



Accepted Manuscript

Downloaded from https://academic.oup.com/jxb/advance-article-abstract/doi/10.1093/jxb/eraa167/5815313 by guest on 07 April 2020

**GUS staining analysis.**

Fragments of the *RAD23B* promoter (-1449 to +826 bp from the translation start site) were amplified from genomic DNA by PCR using primers *RAD23B-p*R and *RAD23B-p*F (Table S1). The fragments were then sub-cloned into the empty vector pDONR207 using BP Clonase for downstream sequencing analysis. Positive fragments were cloned into the destination vector *GW-GUS* using LR Clonase, and were then transformed into *Agrobacterium tumefaciens* GV3101 by electroporation for gene delivery into the *Arabidopsis thaliana* plants using the floral dip method. The transgenic plants were screened using the herbicide basta to identify homozygous transgenic lines. Tissues from the homozygous plants were stained with GUS stain solution as previously described (Jefferson *et al.,* 1986). Then, the photos were taken under a dissecting microscope.

**Hematoxylin staining.**

As described previously, paraffin cross-sectioned samples were analyzed using hematoxylin (Fischer *et al.,* 2008). The sections were dewaxed and incubated with 10% $H_2O_2$ for 10 min. Dip the slide into a Coplin jar containing Mayer's hematoxylin and agitate for 30 seconds. Dehydrate the sections with two changes of 95% alcohol and examined with a Nikon electron microscope (TE2000).

***In vitro* pollen germination analysis.**

Pollen germination analysis was performed as follows (Fan *et al.,* 2001): Fifty flowers were randomly collected from different mutant and WT plants. The anthers were carefully dipped in 1.5 ml microtubes or Eppendorf microtubes with 700 µl germination liquid, oscillated for 2-3 min, transferred to a new microtube or Eppendorf microtube, and collected using centrifugation at 12,000 g for 2 min. Pollen grains were resuspended in liquid germination medium (GM) and cultured in semi-solid germination media (GM supplemented with 0.5% agarose), in a chamber at 23°C with 100% relative humidity. The germinated pollen grains of mutants and WT were counted under a Nikon microscope (TE2000) after 8 h incubation. Each value was obtained from three independent experiments (n=150-200), and data represent the means (± SD).

**Yeast Two-Hybrid analysis.**

The yeast two-hybrid (Y2H) analysis was performed as previously described (Du *et al.,* 2016). Briefly, the full length of RAD23-B was amplified using primers (see in Table S1) and sub-cloned in-frame with GAL4D-AD (pGADT7) as a bait. The KRP1 coding sequence was inserted into GAL4D-BD (pGBKT7) as a prey in the same manner. The bait and prey vectors were transfected into the yeast



Accepted Manuscript

Downloaded from https://academic.oup.com/jxb/advance-article-abstract/doi/10.1093/jxb/eraa167/5815313 by guest on 07 April 2020

strain AH109 to create the GAL4-based Y2H system. Colonies were selected and grown in the absence of histidine, but in the presence of 10 mM 3-AT (Sigma, U.S.). (Then, the photos were taken after 5-7 days.)

***In vitro* GST Pull-down analysis.**

A GST pull-down assay was conducted as previously described (Du *et al.,* 2016) with minor modifications. The coding sequence of *RAD23B* was cloned into the pGEX4T-1 vector, and the coding sequences of KRPs were sub-cloned into the pET28b vector. The specific primers used here are described in the Table 1. His-KRPs proteins were incubated with GST and GST-RAD23B Glutathione Agarose (40 µl, Thermo) at 4°C for 2 h, respectively. 5% mixture was extracted for input. Glutathione Agarose was washed five times with PBS. Bound proteins were eluted from the beads with 40 µl of Elution Buffer (50 mM Tris-Cl, 300 mM NaCl, 20 mM reduced glutathione pH 8). The resulting isolated proteins were detected by immunoblot analysis using anti-His and anti-GST antibodies as primary antibodies, respectively.

**Bimolecular Fluorescence Complementation (BiFC)**

For the BiFC assay, the coding sequence of *RAD23B* was cloned into the pE3308 vector, and the coding sequences of *KRP1* were sub-cloned into the pE3449 vector. The primers for cloning are presented in Table S1. The constructed plasmids were co-transfected into the protoplasts, which were isolated from 4-weeks-old *Arabidopsis* rosette leaves through cellulase and macerozyme digestion. The follow transformation method was performed, as previously described (Li *et al*., 2018), and the co-transfected protoplasts were incubated in the dark at 22°C for 18 hours to allow for the expression of the BiFC proteins. The fluorescence was detected using a confocal microscope (Nikon confocal laser scanning microscope), with wavelengths of 488 nm for GFP.

**Alexander's and DAPI staining analysis.**

For monitoring the pollen development, the different stages pollen grains of mutants were stained using DAPI and Alexander's (Alexander, 1969; Park *et al.,* 1998). Briefly, pollen grains were separated from stamens, and were subsequently stained using Alexander's solution (10% alcohol, 25% glycerol, 4% glacial acetic acid, 500 mg/ml phenol, 500 mg/ml chloral hydrate, 0.5 mg/ml acid fuchsin, and 0.05 mg orange G) for 30 min, and examined under a microscope. In addition, pollen grains were incubated with DAPI staining solution (0.1M sodium phosphate, 1mM EDTA 0.1% Triton X-100, 0.4 µg/ml DAPI; pH 7, Sigma) and maintained in dark conditions for 5 min, prior to examination of pollen grains by fluorescence microscopy.



Accepted Manuscript

Downloaded from https://academic.oup.com/jxb/advance-article-abstract/doi/10.1093/jxb/eraa167/5815313 by guest on 07 April 2020

**Detection of protein degradation *in vivo*.**

The different mutants were grown on 0.5X MS medium for 7 days. Samples were then treated with 40 μM MG132 for 12 h. Total protein was extracted using NEB-T buffer (50 mM HEPES, 40 mM KCl, 5 mM $MgCl_2$, and 1% Triton X-100; pH7.5). The extracts were centrifuged at 12,000 g for 20 min at 4℃ and the supernatants were tested by western blot analysis. Protein bands were detected by immunoblot analysis using anti-Myc and anti-β-actin antibodies as primary antibodies, respectively.

**Results**

***RAD23B* involves in the regulation of pollen grain development.**

To study the expression pattern of *RAD23B*, the construct with a β-glucuronidase (GUS) reporter gene driven by the *RAD23B* promoter was introduced in wide-type Col-0 plants (Figure 1A). By randomly selecting seven GUS transgenic lines for *RAD23B* expression pattern analysis, we found that the GUS signal was clearly detected in the young leaves (Figure 1B), especially in the anthers, and specifically in pollen grains (Figure 1C), while GUS signal in the petals, sepals, and pistil tissues were weak or undetectable (Figure 1D). To examine the biological function of *RAD23B*, knock-outs for homozygous T-DNA insert mutants obtained from ABRC were first identified by PCR (Figure 2A and 2B) and further confirmed by semi-quantitative RT-PCR (Koo et al., 2013). Compared to wild-type plant (Col-0), the expression of *RAD23B* gene was not detectable in the two T-DNA mutants (Figure 2C), indicating that the T-DNA insertions truly disrupted expression of *RAD23B* and *rad23b-1 and rad23b-2* are both null mutants. To obtain *RAD23B* overexpression plants, Col-0 plants were transformed with a full length *RAD23B* coding sequence driven by the CaMV35S promoter (Col-0/*35S::RAD23B-Myc*). Two positive transgenic lines were confirmed by western blot, showing high expression levels of RAD23B (Figure 2D). In addition, *rad23b-1* mutant was transformed with the same overexpression construct (*rad23b-1/35S::RAD23B-Myc*) and positive plants were selected for subsequent experiments. Since *RAD23B* was expressed in pollen grains, its role in cell cycle regulation of pollen grains was followed at different developmental stages with hematoxylin staining (Fischer *et al.*, 2008). We found that the microspores of *rad23b-1* mutant at the G1-S transcription displayed no detectable defects but became much more vacuolated than Col-0 at the binuclear cell stage (Figure 2E). At the G2-M transcription, the *rad23b-1* mutant showed increased number of microspore vacuolizations. In addition, overexpression of *RAD23B* (*rad23b-1/35S::RAD23B-Myc*) was capable of completely rescuing vacuolization defects in *rad23b-1* mutant plants



Accepted Manuscript

Downloaded from https://academic.oup.com/jxb/advance-article-abstract/doi/10.1093/jxb/eraa167/5815313 by guest on 07 April 2020

(Figure 2E). Taken together, the data suggest that *RAD23B* plays an important role in the cell cycle regulation of pollen grains. In addition, pollen germination were also investigated in Col-0, *rad23b-1* mutant, *rad23b-1/35S::RAD23B*, and Col-0/*35S::RAD23B* plants. The results indicated that pollen grain germination rates of Col-0, *rad23b-1* mutant, overexpression lines, and *rad23b-1/35S::RAD23B* were 91.7%, 61.6%, 91.4% and 91.9%, respectively (Figure S1). Compared to Col-0, the pollen grain germination rate of *rad23b-1* mutant was significantly lower (Figure S1). More importantly, *rad23b-1/35S::RAD23B* was able to fully rescue pollen germination phenotype which strongly suggested that the absence of RAB23B was the cause of this developmental phenotype.

**RAD23B interacts with the CDK inhibitor KRP1 through its UBL-UBA domain.**

To better understand the function of the RAD23B protein, the Y2H system was used to screen RAD23B interacting proteins (Du *et al.,* 2016). One cyclin-dependent kinase inhibitor, KRP1, was observed to interact with RAD23B. To further confirm this interaction, an *in vitro* pull-down assay was used to investigate the interaction of RAD23B with KRPs. Seven of His-KRPs and GST-RAD23B fusion proteins were expressed and purified (Figure S2). We found KRP1 strongly interacted with RAD23B, while KRP6, another cyclin-dependent kinase inhibitor, only weakly interacted with RAD23B (Figure 3A). The constructs were then co-transformed into AH109 yeast cells and selected on synthetic dropout medium to test the interaction. In addition, full length coding sequences of RAD23B and KRP1 were cloned into the pair vectors GAL4D-AD (pGADT7) and GAL4D-BD (pGBKT7) to generate AD-RAD23B and BD-KRP1. Strong interaction was observed as only the cells co-expressed RAD23B and KRP1 can grow in medium without His (Figure 3B). To confirm the *in vivo* interaction, we used a bimolecular fluorescence complementation (BiFC) assay. GFP signal can be detected when RAD23B-nVenus and KRP1-CFP were co-expressed (Figure 3C). These data reinforced a conclusion that RAD23B physically interacts with KRP1 *in vitro* and *in vivo*. To investigate which domain contribute to the interaction between RAD23B and KRP1, RAD23B-L (that lacks UBL domain), RAD23B-U (lacking one UBA domain), RAD23B-US (that lacks one UBA domain and the STI1 domain) and RAD23B-USU (that lacks UBA domains and the STI1 domain) were cloned into GAL4D-AD (pGADT7) vector and transformed into AH109 yeast cells to test the interaction with KRP1 (Figure 3D). Full length RAD23B was used as a positive control. We observed that KRP1 interacted with RAD23B only when both UBL and UBA domains of RAD23B were present, which indicated that the UBL-UBA domains of RAD23B are essential for the KRP1-RAD23B interaction.

Accepted Manuscript

Downloaded from https://academic.oup.com/jxb/advance-article-abstract/doi/10.1093/jxb/eraa167/5815313 by guest on 07 April 2020

**RAD23B contributes to KRP1 degradation through 26S proteasome-dependent proteolysis.**

RAD23B, a UBL/UBA protein, functioned as a hub during ubiquitin-mediated protein degradation (Steven *et al.,* 2011). We found RAD23B could directly interact with KRP1. Therefore, we hypothesized RAD23B contributed to KRP1 degradation. To test this hypothesis, we measured the protein levels of *KPR1* in Col-0 and in *rad23b-1* mutant. It was found that KRP1 protein levels significantly increased in the absence of RAD23B protein (in *rad23b-1* mutant, Figure 4A). To exclude the possibility that increasing of KRP1 protein level in *rad23b-1* was due to deregulation of *KRP1* transcript, we examined the gene expression level of *KRP1* in WT and *rad23b-1* mutant (Figure 4B). The change between WT and *rad23b-1* mutant is almost negligible. Furthermore, the accumulation of KRP1 protein level in the wild-type can be mimicked in *rad23b* mutant following treatment with MG132, a proteasome inhibitor (Figure 4C), while gene expression level of *KRP1* remain undisturbed (Figure 4D). Taken together, we found that the intracellular level of KRP1 protein was regulated by RAD23B through 26S proteasome-dependent proteolysis.

**Overexpression of KRP1 mimics the phenotype of *rad23b* mutant plants.**

Our previous results showed that the *rad23b-1* mutant was defective in pollen development and the RAD23B protein can directly interact with KRP1. Therefore, it is reasonable to suspect that KRP1 was also involved in regulation of pollen development. Two independent lines of KRP1 overexpression transgenic plants (*35S::KRP1-Myc*) were confirmed by western blot (Figure 5A). For further analysis, we used *35S::KRP1-Myc* line-2 as it showed highest protein level. The male gametogenesis was investigated for Col-0/*35S::KRP1-Myc-2*, Col-0, and *rad23b-1* plants using Alexander's staining and DAPI staining (Alexander, 1969; Park et al., 1998). The result showed that the microspores of the *rad23b-1* and Col-0/*35S::KRP1-Myc-2* exhibit no difference compared to wild-type at the G1-S transition stage (Figure S3). During the G2-M transition, both the *rad23b-1* mutant and Col-0/*35S::KRP1-Myc-2* produced more microspores vacuolization than wild-type (Figure 5B). The microspores vacuolization rates of the WT, *rad23b* mutant, Col-0/*35S::KRP1-Myc-2* lines were 0.3%, 13.4% and 16.8% in bicellular pollen stage and 0.3%, 50.6% and 60.3% in tricellular pollen stage, respectively (Figure 5C). These results show that the overexpression of *KRP1* could mimic the phenotype of *rad23b-1* mutant, suggesting that both *KRP1* and *RAD23B* play an important role in cell division during pollen grain development.

Accepted Manuscript

Downloaded from https://academic.oup.com/jxb/advance-article-abstract/doi/10.1093/jxb/eraa167/5815313 by guest on 07 April 2020

**Discussion**

In eukaryotes, protein ubiquitination and degradation play critical roles in the cell cycle regulation by destroying important cell cycle regulatory molecules (Liu *et al.,* 2008; Cross *et al.,* 2011). Among the various identified CKIs, proteins of the UBL/UBA family including RPN1, RPN10, and RPN13 (Brukhin *et al.,* 2005; Isasa *et al.,* 2010; Besche *et al.,* 2014; Hamazaki *et al.,* 2015), as well as RAD23 and DSK2, are believed to target and deliver poly-ubiquitin substrates to the proteasome. Here, we demonstrated that RAD23, a member of UBL/UBA family, increased the degradation of KRP1 during the cell G2-M transition through directly interacting with each other. Genetic analysis also suggested that the mutant of *rad23b* exhibits a similar phenotype to KRP1 overexpression plants. Taken together, these data provided compelling evidence that RAD23B is involved in the regulation of KRP1, and accordingly, affected the cell cycle regulation.

Similar to other eukaryotes, plants express many UBL/UBA proteins, which are orthologous to yeast proteins, such as RAD23, DSK2, and DDI1 (Díaz-Martínez *et al.,* 2006). The proteins possess similar structures, an N-terminal UBL domain and one or more C-terminal UBA domains (Liang *et al.,* 2014). UBL/UBA proteins are also likely to participate in many developmental events in plants, including cell cycle regulation, DNA repair, and regulation of transcription (Mueller and Smerdon, 1996; Emilie *et al.,* 2009; Zhang *et al.,* 2012). Recent studies indicate that RAD23 binds some Ub conjugates, particularly through directly interacting with the 26S proteasome Ub receptor RPN10, and is involved in protein degradation (Smalle *et al.,* 2003). Another study reported that *rad23b* mutants exhibited a marked seed abortion phenotype (Farmer *et al.,* 2010). Earlier studies showed that KRP1 overexpression line displayed shorter siliques and fertility defects, which is similar to phenotype of *rad23b* mutants (Ren *et al.,* 2008). The authors speculated that RAD23 might promote the degradation of one or more cell cycle proteins in order to regulate plant development (Farmer *et al.,* 2010). Here, we demonstrated that the *RAD23B* gene was highly expressed during the G1-S transition phase of the cell cycle, the expression level was even higher during the G2-M transition. In addition, knockout lines of *RAD23B* resulted in a pronounced pollen abortion during the G2-M transition phase and this phenotype can be rescued by overexpression of *RAD23B-Myc*. Taken together, these data indicated that RAD23B was likely to be involved in the regulation of plant cell cycle.

In yeast and animals, SCF complex is a critical component for cell division regulation. SCF complex targets CKIs to the proteasome for degradation (Patton *et al.,* 1998). It has also been reported that CDKA;1/CYCD2;1 plays a critical role in the G1-S transition (Churchman *et al.,* 2006; Hirano *et al.,* 2011). Furthermore, the KRP1 protein has been demonstrated to interact directly with CDKA;1/CYCD2;1 *in vivo* (Yan *et al.,* 2015; Vieira *et al.,* 2017), which strongly suggests the crucial



Accepted Manuscript

Downloaded from https://academic.oup.com/jxb/advance-article-abstract/doi/10.1093/jxb/eraa167/5815313 by guest on 07 April 2020

functions of KRP1 in the regulation of the G1-S transition. Interestingly, Weinl *et al.* reported that KRP1 also played an important role in the G2-M transition to regulate the entry into mitosis (Weinl *et al.,* 2005), although a detailed understanding of the mechanisms is lacking. Here, we demonstrated that RAD23B interacted directly with KRP1 *in vivo* and *in vitro* while *rad23b* mutants exhibited an increased frequency of abnormal microspores during the G2/M transition phase. Similarly, this phenotype can also be observed in the KRP1 overexpression line. Furthermore, genetic evidence suggested that RAD23B also contributed to the degradation of KRP1. RAD23B promoted KRP1 degradation, thus KRP1 protein was more stable in *rad23b* mutant. Accumulation of KRP1 protein in the wild-type following treatment with MG132 suggested that RAD23 mediated the degradation of KRP1 through trafficking of the substrates to the proteasome. Taken together, our data indicated that RAD23B protein functioned as a negative regulator of KRP1 to modulate cellular division in pollen grain development.

Accepted Manuscript

Downloaded from https://academic.oup.com/jxb/advance-article-abstract/doi/10.1093/jxb/eraa167/5815313 by guest on 07 April 2020

**Acknowledgements**

This research is financially supported by the National Science Foundation of China (Nos. 31571635, 31871595), Hunan Provincial Important Science and Technology Specific Projects (No. 2018NK1010), and Planned Science and Technology Project of Changsha City (Nos. kq1801001). This work was also supported by grants from ANPCyT (PICT2016-0132 and PICT2017-0066), ICGEB CRP/ARG16-03, and Instituto Milenio iBio – Iniciativa Científica Milenio, MINECON to J.M.E.

Accepted Manuscript

Downloaded from https://academic.oup.com/jxb/advance-article-abstract/doi/10.1093/jxb/eraa167/5815313 by guest on 07 April 2020

## References


**Alexander MP.** 1969. Differential staining of aborted and nonaborted pollen. *Stain Technology* **44,** 117-122.

**Andersson HA, Passeri MF, Barry MA.** 2005. Rad23 as a reciprocal agent for stimulating or repressing immune responses. *Human Gene Therapy* **16,** 634–641.

**Bergink S, Theil AF, Toussaint W, Cuyper IMD, Kulu DI, Clape T, Linden RVD, Demmers JA, Mul EP, Alphen FPV, Marteijn JA, Gent TV, Maas A, Robin C, Philipsen S, Vermeulen W, Mitchell JR, Gutiérrez L.** 2013. Erythropoietic defect associated with reduced cell proliferation in mice lacking the 26S proteasome shuttling factor Rad23b. *Molecular and Cellular Biology* **33,** 3879–3892.

**Besche HC, Sha Z, Kukushkin NV, Peth A, Hock EM, Kim W, Gygi S, Gutierrez JA, Liao H, Dick L, Goldberg AL.** 2014. Autoubiquitination of the 26S proteasome on Rpn13 regulates breakdown of ubiquitin conjugates. *The EMBO Journal* **33,** 1159–1176.

**Bird DA, Buruiana MM, Zhou YM, Fowke LC, Wang, H.** 2007. *Arabidopsis* cyclin-dependent kinase inhibitors are nuclear-localized and show different localization patterns within the nucleoplasm. *Plant Cell Report* **26,** 861–872.

**Brukhin V, Gheyselinck J, Gagliardini V, Genschik P, Grossniklaus U.** 2005. The RPN1 subunit of the 26S proteasome in *Arabidopsis* is essential for embryogenesis. *The Plant Cell* **17,** 2723–2737.

**Cheng Y, Liu H, Cao L, Wang S, Li YP, Zhang YY, Jiang W, Zhou YM, Wang H.** 2015. Down-regulation of multiple CDK inhibitor ICK/KRP genes promotes cell proliferation, callus induction and plant regeneration in *Arabidopsis*. *Frontiers in Plant Science* **6,** 825-837.

**Churchman ML, Brown ML, Kato N, Kirik, V, Hu¨lskamp M, Inze´ D, Veylder LD, Walker JD, Zheng ZG, Oppenheimer DG, Gwin T, Churchman J, Larkin JC.** 2006. SIAMESE, a plant-Specific cell cycle regulator, controls endoreplication onset in *Arabidopsis thaliana*. *The Plant Cell* **18,** 3145–3157.

**Clough SJ, Bent AF.** 1998. Floral dip: a simplified method for Agrobacterium-mediated transformation *Arabidopsis thaliana*. *The Plant Journal* **16,** 735–743.

**Cross FR, Buchler NE, Skot JM.** 2011. Evolution of networks and sequences in eukaryotic cell cycle control. *Philosophical Transactions of the Royal Society B* **366,** 3532-3544.

**Díaz-Martínez LA, Kang Y, Walters KJ, Clarke DJ.** 2006. Yeast UBL-UBA proteins have partially redundant functions in cell cycle control. *BioMed Central Cell Division* **1,** 28-39.

**Ding QJ, Jiang N, Chu XJ, Lovey A, Depinto W, Vu B, Bartkovitz D, Mullin J, Kaplan G, Moliterni J, Packman K, Smith M, So SS, Graves B, Lukacs C, Yin XF, Chen YS.** 2005. Design, synthesis of 1,4-cyclohexyldiamine substituted diaminopyrimidines as selective inhibitors of CDK1, CDK2 and CDK4 and their *in vitro* and *in vivo* evaluation. *Cancer Research* **46,** 4414.

**Du CQ, Li XS, Chen J, Chen WJ, Li B, Li CY, Wang L, Li JL, Zhao XY, Lin JZ, Liu XM, Luan S, Yu F.** 2016. Receptor kinase complex transmits RALF peptide signal to inhibit root growth in *Arabidopsis*. *Proceedings of the National Academy of Sciences of the United States of America* **113,** E8326-E8334.




Downloaded from https://academic.oup.com/jxb/advance-article-abstract/doi/10.1093/jxb/eraa167/5815313 by guest on 07 April 2020

**Du Z, Zhou X, Li L, Su Z.** 2009. PlantsUPS: a database of plants' Ubiquitin Proteasome System. *BioMed Central Genomics* **10,** 227-233.

**Fan LM, Wang YF, Wang H.** 2001. *In vitro Arabidopsis* pollen germination and characterization of the inward potassium currents in *Arabidopsis* pollen grain protoplasts. *Journal of Experimental Botany* **52,** 1603-1614.

**Farmer LM, Book AJ, Lee KH, Lin YL, Fu HY, Vierstra RD.** 2010. The RAD23 family provides an essential connection between the 26S proteasome and ubiquitylated proteins in *Arabidopsis*. *The Plant Cell* **22,** 124–142.

**Fischer AH, Jacobson KA, Rose J, Zeller R.** 2008. Hematoxylin and eosin staining of tissue and cell sections. *Cold Spring Harbor Protocols* **10,** 4986.

**Haase SB, Wittenberg C.** 2013. Topology and control of the cell-cycle-regulated transcriptional circuitry. *Genetics* **196,** 65–90.

**Hamazaki J, Hirayama S, Murata S.** 2015. Redundant roles of Rpn10 and Rpn13 in recognition of ubiquitinated proteins and cellular homeostasis. *The Public Library of Science Genetics* **11,** e1005401-e1005421.

**Hänzelmann P, Stingele J, Hofmann K, Schindelin H, Raasi S.** 2010. The yeast E4 ubiquitin ligase Ufd2 interacts with the ubiquitin-like domains of Rad23 and Dsk2 via a novel and distinct ubiquitin-like binding domain. *The Journal of Biological Chemistry* **285,** 20390–20398.

**Hiran H, Shinmyo A, Sekine M.** 2011. Both negative and positive G 1 cell cycle regulators undergo proteasome-dependent degradation during sucrose starvation in *Arabidopsis*. *Plant Signaling & Behavior* **6,** 1394-1396.

**Isasa M, Katz EJ, Kim W, Yugo V, Gonza´lez S, Kirkpatrick DS, Thomson TM, Finley D, Gygi SP, Crosas B.** 2010. Monoubiquitination of RPN10 regulates substrate recruitment to the proteasome. *Molecular Cell* **38,** 733–745.

**Jefferson R, Burgess S, Hirsh D.** 1986. ß-glucuronidase from escherichia coli as a gene-fusion marker. *Proceedings of the National Academy of Sciences of the United States of America* **83,** 8447-8451.

**Kurepa J, Wang SH, Li Y, Zaitlin D, Pierce AJ, Smalle JA.** 2009. Loss of 26S Proteasome Function Leads to Increased Cell Size and Decreased Cell Number in *Arabidopsis* Shoot Organs. *Plant Physiology* **150,** 178–189.

**Lai JB, Chen H, Teng KL, Zhao QZ, Zhang ZH, Li Y, Liang LM, Xia R, Wu YR, Guo HS, Xie Q.** 2009. RKP, a RING finger E3 ligase induced by BSCTV C4 protein, affects geminivirus infection by regulation of the plant cell cycle. *The Plant Journal* **57,** 905–917.

**Liang RY, Chen L, Ko BT, Shen YH, Li YT, Chen BR, Lin KT, Madura K, Chuang SM.** 2014. Rad23 interaction with the proteasome is regulated by phosphorylation of its ubiquitin-like (UBL) domain. *Journal Molecular Biological* **426,** 4049–4060.



Downloaded from https://academic.oup.com/jxb/advance-article-abstract/doi/10.1093/jxb/eraa167/5815313 by guest on 07 April 2020

**Liu JJ, Zhang YY, Qin GJ, Tsuge T, Sakaguchi N, Luo G, Sun KT, Shi DQ, Aki S, Zheng NY, Aoyama T, Oka A, Yang WC, Umeda M, Xie Q, Gu HY, Qu LJ.** 2008. Targeted degradation of the cyclin-dependent kinase inhibitor ICK4/KRP6 by RING-Type E3 ligases is essential for mitotic cell cycle progression during *Arabidopsis* gametogenesis. *The Plant Cell* **20,** 1538–1554.

**Liu H, Ma X, Han HN, Hao YJ, Zhang XS.** 2016. AtPRMT5 regulates shoot regeneration through mediating histone H4R3 dimethylation on KRPs and pre-mRNA splicing of RKP in *Arabidopsis*. Molecular Plant **9,** 1634-1646.

**Lowe ED, Hasan N, Trempe JF, Fonso L, Noble MEM, Endicott JA, Johnson LN, Brown NR.** 2006. Structures of the Dsk2 UBL and UBA domains and their complex. *Acta Crystallographica* **62,** 177–188.

**Medina B, Paraskevopoulos K, Boehringer J, Sznajder A, Robertson M, Endicott J, Gordon C.** 2012. The ubiquitin-associated (UBA) 1 domain of schizosaccharomyces pombe Rhp23 is essential for the recognition of ubiquitin-proteasome system substrates both in vitro and in vivo. *The Journal of Biological Chemistry* **287,** 42344–42351.

**Mueller JP, Smerdon MJ.** 1996. Rad23 is required for transcription-coupled repair and efficient overall repair in saccharomyces cerevisiae. *Molecular and Cellular Biology* **16,** 2361–2368.

**Park SK, Howden R, Twell D.** 1998. The *Arabidopsis thaliana* gametophytic mutation gemini pollen1 disrupts microspore polarity, division asymmetry and pollen cell fate. *Development* **125,** 3789–3799.

**Patton EE, Willems AR, Sa D, Kuras L, Thomas D, Craig KL, Tyers M.** 1998. Cdc53 is a scaffold protein for multiple Cdc34/Skp1/F-box protein complexes that regulate cell division and methionine biosynthesis in yeast. *Genes & Development* **12,** 692–705.

**Peng J, Yu DS, Wang LQ, Xie M, Yuan CY, Wang Y, Tang DY, Zhao, XY, Liu, XM.** 2012. *Arabidopsis* F-box gene *FOA1* involved in ABA signaling. *Science China Life Science*s **55,** 497-506.

**Ren H, Santner A, Pozo JCD, Murray JAH, Estelle M.** 2008. Degradation of the cyclin-dependent kinase inhibitor KRP1 is regulated by two different ubiquitin E3 ligases. *The Plant Journal* **53,** 705–716.

**Renaud E, Miccoli L, Zacal N, Biard DS, Craescu CT, Rainbow AJ, Angulo JF.** 2011. Differential contribution of XPC, RAD23A, RAD23B and CENTRIN 2 to the UV-response in human cells. *DNA Repair* **10,** 835– 847.

**Shen H, Moon J, Huq E.** 2005. PIF1 is regulated by light-mediated degradation through the ubiquitin-26S proteasome pathway to optimize photomorphogenesis of seedlings in *Arabidopsis*. *The Plant Journal* **44,** 1023–1035.

**Smalle J, Kurepa J, Yang P, Emborg TJ, Babiychuk E, Kushnir S, Vierstra RD.** 2003. The pleiotropic role of the 26S proteasome subunit RPN10 in *Arabidopsis* growth and development supports a substrate-specific function in abscisic acid signaling. *The Plant Cell* **15,** 965–980.

**Veylder LD, Beeckman T, Beemster GTS, Krols L, Terras F, Landrieu I, Schueren EVD, Maes S, Naudts M, Inzé D.** 2001. Functional analysis of cyclin-dependent kinase inhibitors of *Arabidopsis*. *The Plant Cell* **13,** 1653–1667.



Downloaded from https://academic.oup.com/jxb/advance-article-abstract/doi/10.1093/jxb/eraa167/5815313 by guest on 07 April 2020

**Vieira P, Engler JDA.** 2017. Plant cyclin-dependent kinase inhibitors of the KRP family: potent inhibitors of root-knot nematode feeding sites in plant roots. *Frontiers in Plant Science* **8,** 1514-1523.

**Weinl C, Marquardt S, Kuijt SJH, Nowack MK, Jakoby MJ, Hu¨lskamp M, Schnittger A.** 2005. Novel functions of plant cyclin-dependent kinase inhibitors, ICK1/KRP1, can act non-cell-autonomously and inhibit entry into mitosis. *The Plant Cell* **17,** 1704–1722.

**Zhang JH, Guo XH, Li XS, Xiang F, Zhou B, Yu DS, Tang DY, Liu XM.** 2012. The genetic and physiological analysis of late-flowering phenotype of T-DNA insertion mutants of *AtCAL1* and *AtCAL2* in *Arabidopsis*. *Molecular Biology Reports* **39,** 1527-1535.

**Zhang YH, Zhang MS, Wu JC, Lei GH, Li HL.** 2012. Transcriptional regulation of the ufm1 conjugation system in response to disturbance of the endoplasmic reticulum homeostasis and inhibition of vesicle trafficking. *The Public Library of Science One* **7,** e48587- e48598.

Accepted Manuscript

Downloaded from https://academic.oup.com/jxb/advance-article-abstract/doi/10.1093/jxb/eraa167/5815313 by guest on 07 April 2020

**Figure Legends**

**Figure 1. Expression patterns of *RAD23B* in Arabidopsis plants.**

(A) Map of construct for GUS staining to investigate *RAD23*B expression pattern.

(B) GUS staining analysis for developing leaves of 6-day-old plantlets. Scale bar = 1 mm.

(C) GUS staining analysis for flower organs of 42-day-old plants. Scale bar = 1 mm.

(D) GUS staining analysis for pollen grains in (C). Scale bar in left= 50 μm, Scale bar in right= 10 μm.

**Figure 2. Lack of RAD23B induces the abortion of pollen grains.**

(A) The RAD23B gene structure as well as the locations of T-DNA insertion in two mutant lines, SALK_075940 (*rad23b-1*) and SALK_130110 (*rad23b-2*).

(B) PCR identification of homozygous lines of T-DNA mutants with various primer combinations. The presence or absence of T-DNA insertions correspond to PCR products from primers R0+RP and LP+RP, respectively.

(C) RAD23B expression in the WT and the two mutant lines for *RAD23B*. ACTIN2 served as an internal control.

(D) Western blotting analysis of WT and two line of Col-0/*35S::RAD23B* transgenic lines, β-Actin as a loading control.

(E) Transverse sections of flowers stained with hematoxylin were examined by light microscopy. Red arrows indicate abortive microspores, and black arrows indicate normal microspores. E, epidermis; En, endothecium; ML, middle layer; T, tapetum; MM, microspore mother cell; Scale bar =5 μm.

**Figure 3. UBL-UBA domains are required for RAD23B interaction with KRP1.**

(A) Pull-down assays of RAD23B-GST and His-KRPs. The complex was separated using SDS/PAGE, and tested by anti-His (Upper) and anti-GST (Lower) primary antibody.

(B) Yeast two-hybrid assay to analyze the interaction between KRP1 and RAD23B on SD Ⅲ agar medium (-Trp, -Leu, -His, +10 mM 3AT).

(C) The RAD23B-cCFP and KRP1-nVenus were co-expressed in the mesophyll protoplasts of *Arabidopsis*. GFP fluorescence was detected in the protoplasts of RAD23B-cCFP+KRP1-nVenus, but not in the control. All experiments were repeated three times. Scale bar =50 μm.

(D) Yeast two-hybrid assay to analyze the interaction between KRP1 and four different domain combinations of RAD23B, RAD23B-L (74 to 395 amino acids), RAD23B-U (1 to 217 amino acids), RAD23B-US (1 to 115 amino acids) and RAD23B-USU (1 to 74 amino acids).

Accepted Manuscript

Downloaded from https://academic.oup.com/jxb/advance-article-abstract/doi/10.1093/jxb/eraa167/5815313 by guest on 07 April 2020

**Figure 4. Effects of RAD23B on the degradation of KRP1 *in vivo*.**

(A)Immunoblots showing KRP1 levels in the absence or presence of RAD23B and Col-0 (WT) as a negative control. Two lines of each transgenic plants are shown. The ratio of Myc/Actin was displayed below the gel, and Actin was shown as a loading control in A and C.

(B) *KRP1* expression in *35S::KRP1-Myc* T2 transgenic plants in WT (lines 3 and 5) and *rad23b-1* backgrounds (lines 1 and 7), respectively. Gene expression determined by quantitative real-time PCR was normalized against the expression of Actin. Data represent the mean ±SD, (n=3).

(C) Immunoblots showing KRP1 levels in the absence or presence of RAD23B with the proteasome inhibitor MG132.

(D) *KRP1* expression in plants in (C) treated with the proteasome inhibitor MG132. Gene expression determined by quantitative real-time PCR was normalized against the expression of Actin. Data represent the mean ±SD, (n=3). ns: not significant in B and D.

**Figure 5. Overexpression of KRP1 causes similar pollen defects than in *rad23b* mutants.**

(A) Western blotting analysis of two Col-0/*35S::KRP1-Myc-3* transgenic lines, Col-0 as a negative control.

(B) DAPI and Alexander's stain of Col-0, *rad23b*, Col-0/*35S::KRP1-Myc* pollen grains at the bicellular and tricellular stage. Yellow arrows indicate abnormal pollen grains with no DAPI staining and the black arrow indicates shrunken pollen grains. Scale bar=25 µm.

(C) Pollen abortion rates were calculated, and each sample was tested in triplicate (n = 100); data represent the mean ±SD. ** is for p-value <0.01.

Accepted Manuscript

Downloaded from https://academic.oup.com/jxb/advance-article-abstract/doi/10.1093/jxb/eraa167/5815313 by guest on 07 April 2020

Figure 1

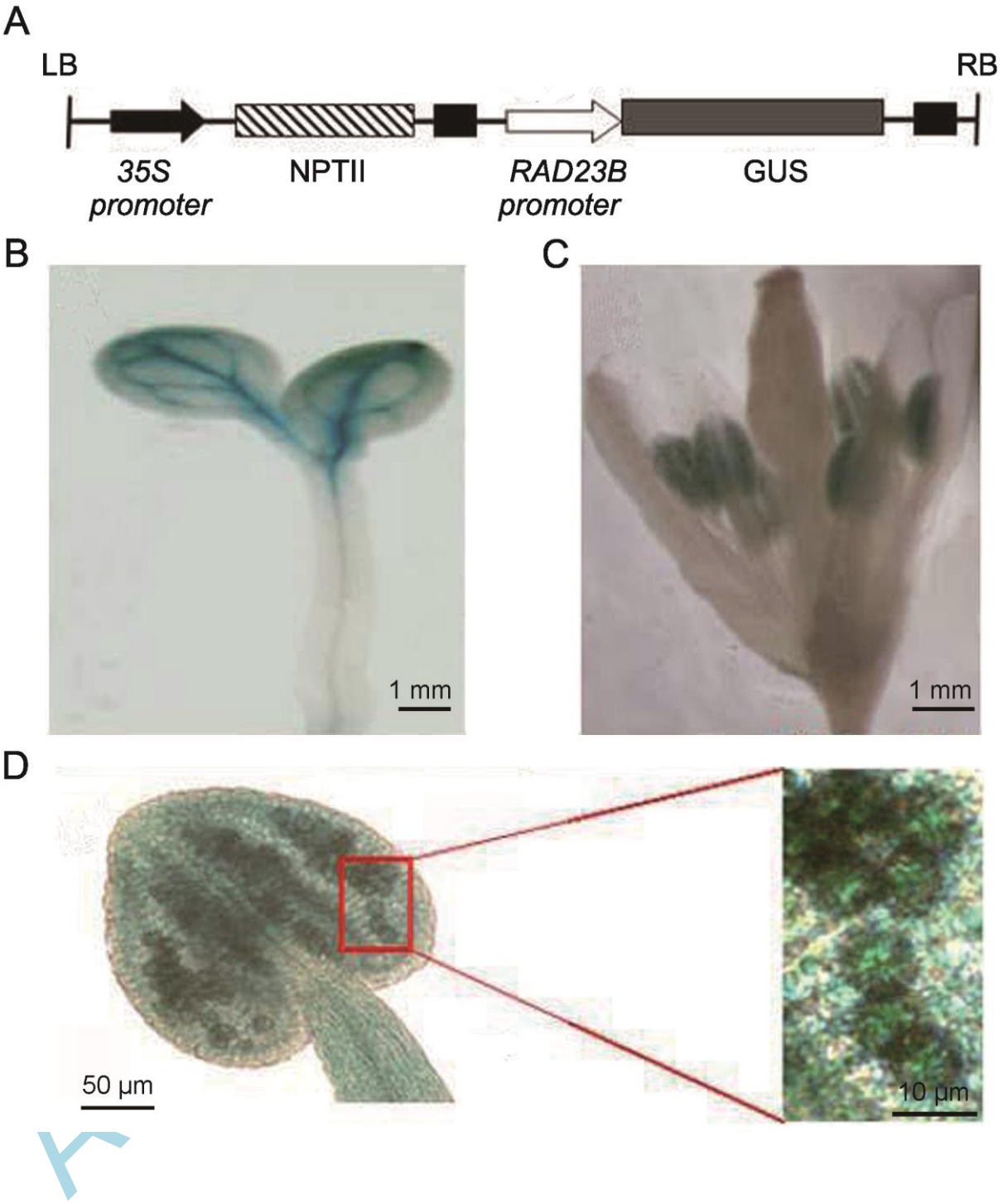


Downloaded from https://academic.oup.com/jxb/advance-article-abstract/doi/10.1093/jxb/eraa167/5815313 by guest on 07 April 2020

Figure 2

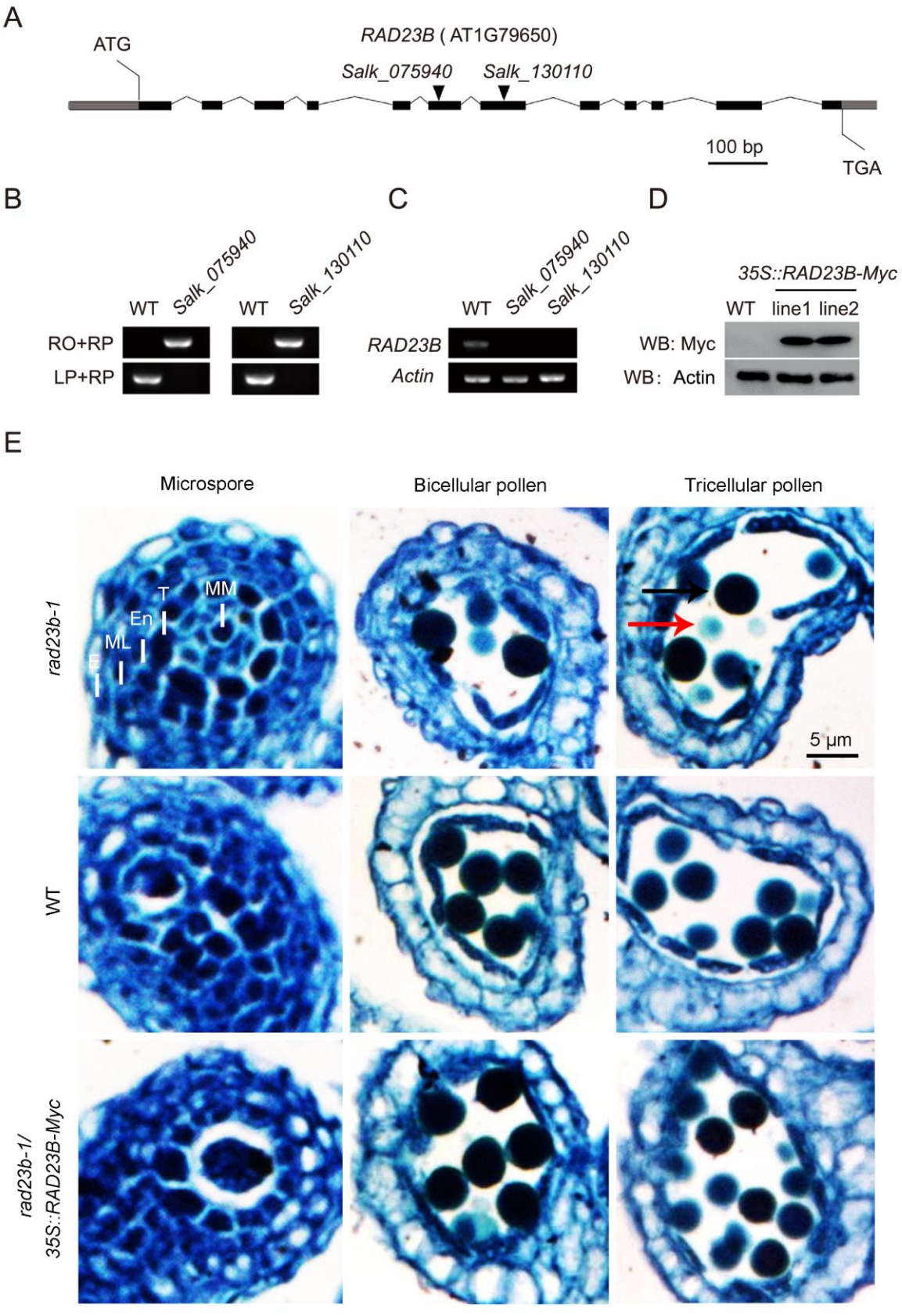


Downloaded from https://academic.oup.com/jxb/advance-article-abstract/doi/10.1093/jxb/eraa167/5815313 by guest on 07 April 2020

Figure 3

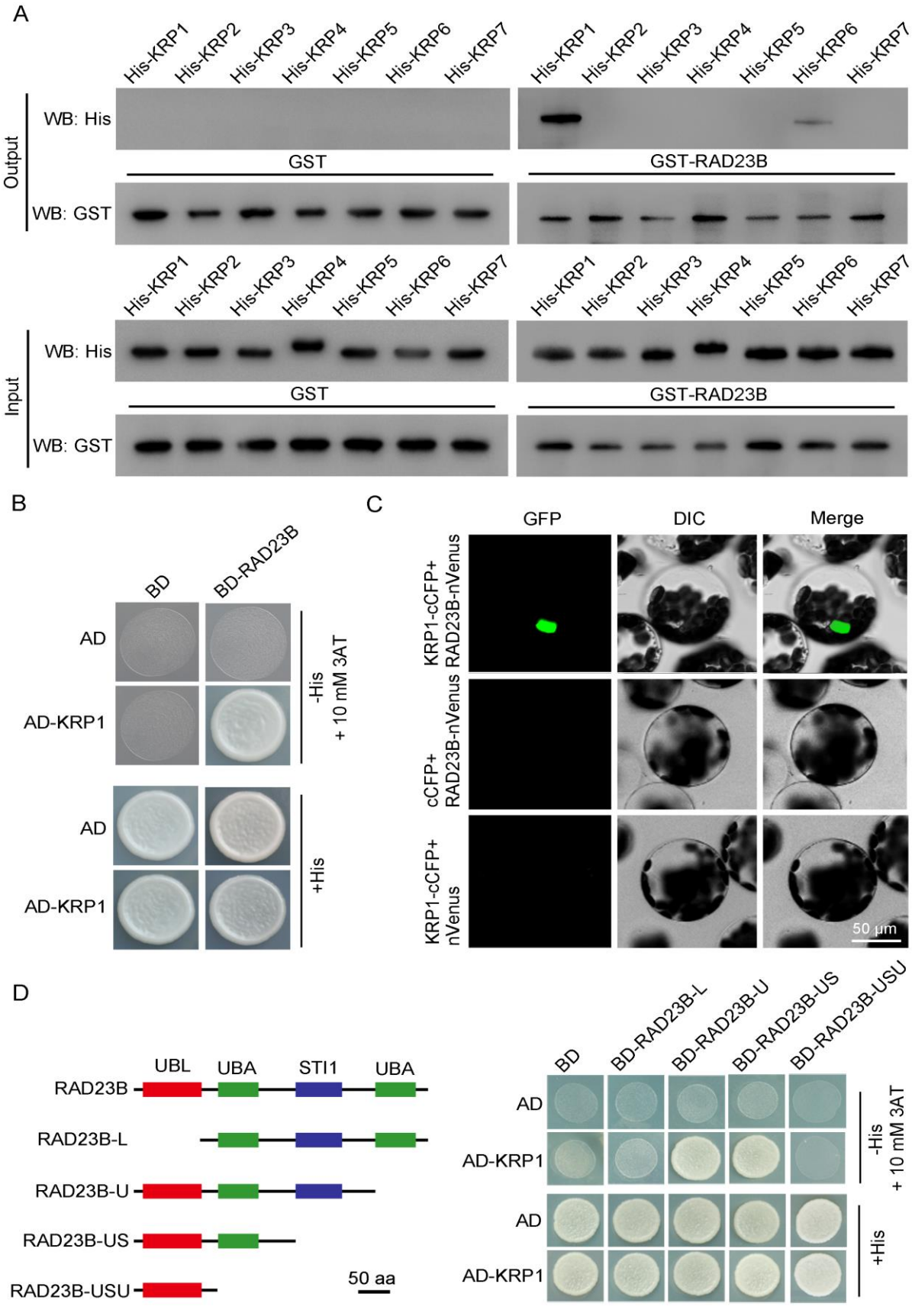


Downloaded from https://academic.oup.com/jxb/advance-article-abstract/doi/10.1093/jxb/eraa167/5815313 by guest on 07 April 2020

Figure 4

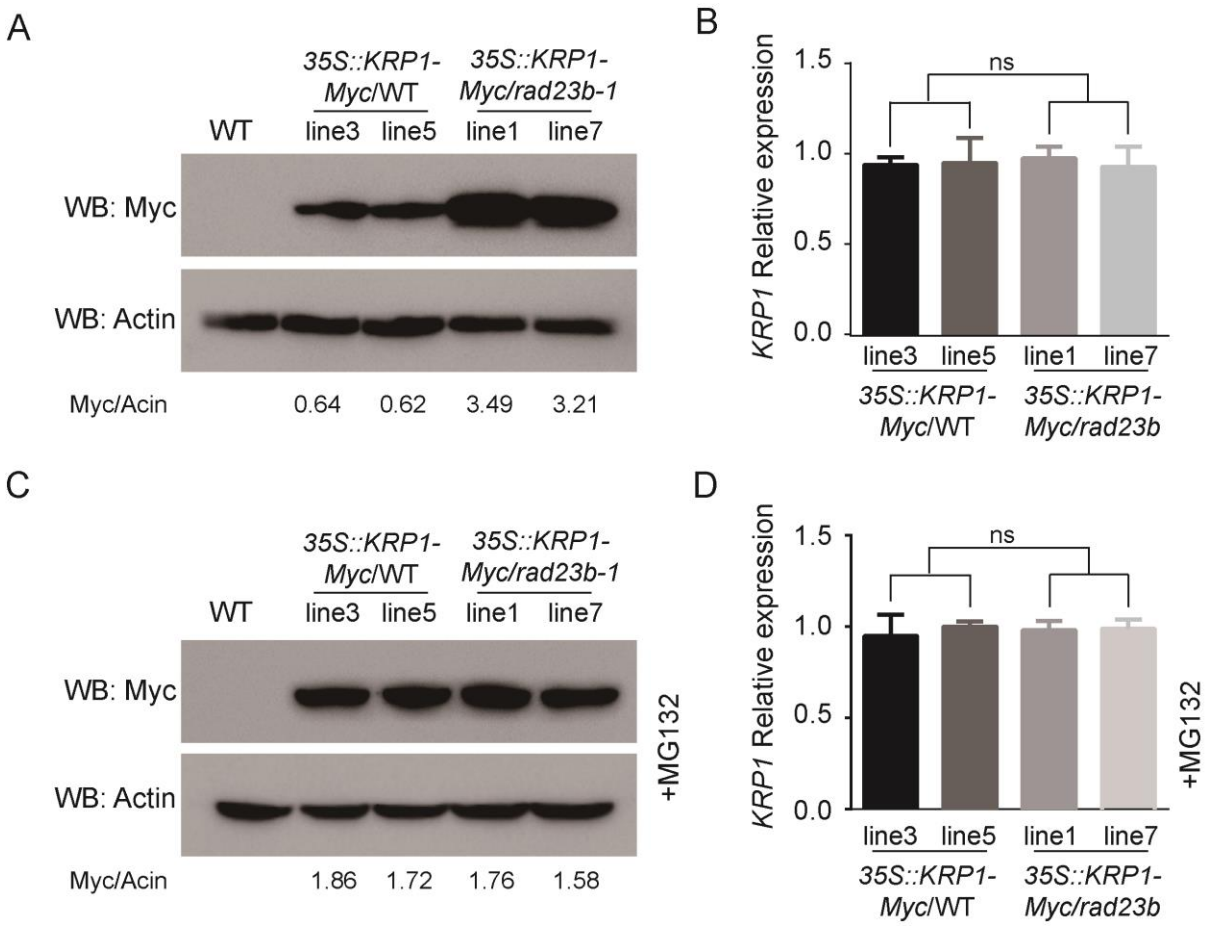


Accepted

Downloaded from https://academic.oup.com/jxb/advance-article-abstract/doi/10.1093/jxb/eraa167/5815313 by guest on 07 April 2020

Figure 5

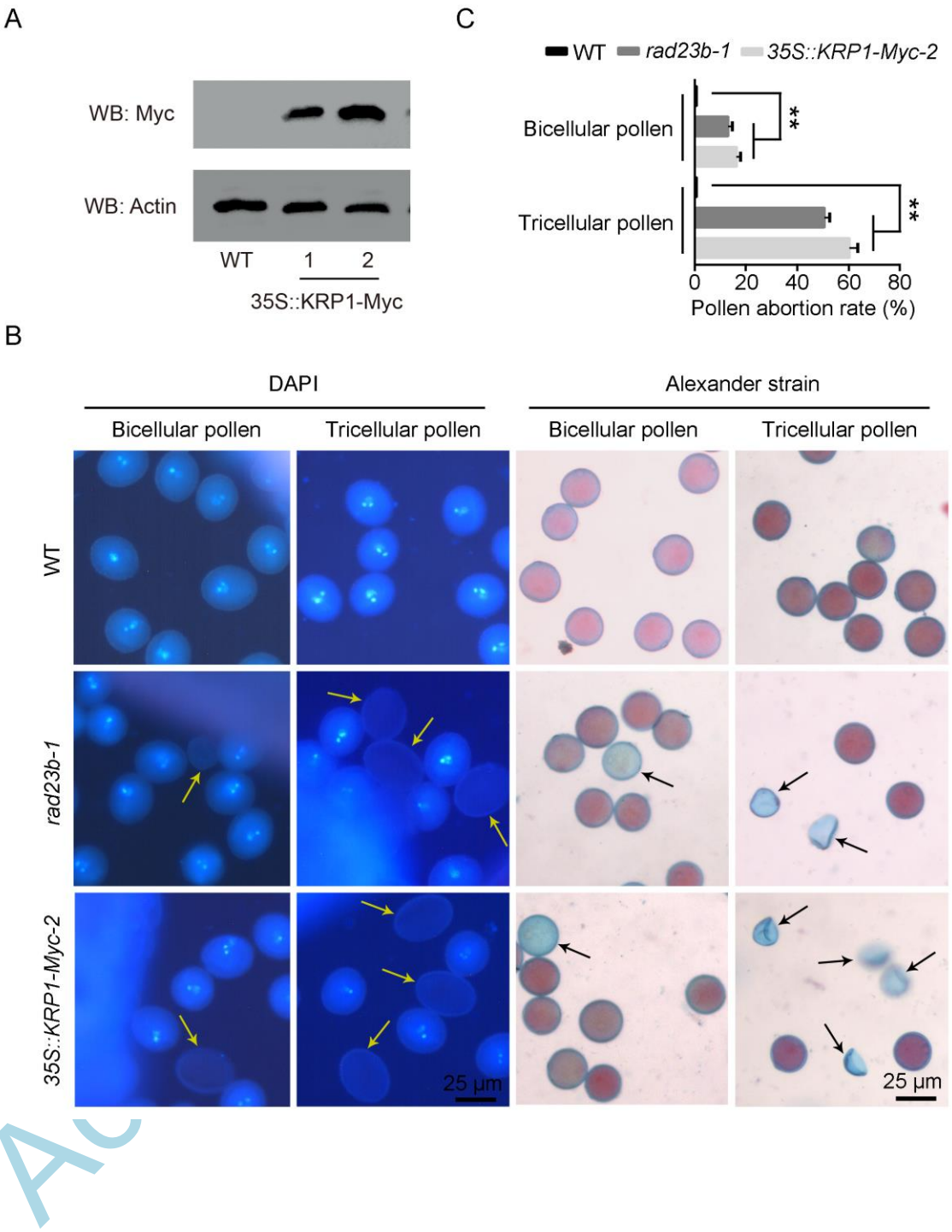


Downloaded from https://academic.oup.com/jxb/advance-article-abstract/doi/10.1093/jxb/eraa167/5815313 by guest on 07 April 2020